Linearized Pitch-Axis Attitude Control of a Rocket Using State Feedback and Observer Design

Blaine Swieder
Department of Electrical and Computer Engineering
Tennessee Technological University
Cookeville, United States
bcswieder42@tntech.edu

Dakota Moye
Department of Electrical and Computer Engineering
Tennessee Technological University
Cookeville, United States
djmoye43@tntech.edu

***Abstract*—In this project, we study pitch-axis control for launch vehicles via a linear state-space model and thrust-vector control under small-angle derivations. We derive a two-state model (pitch angle, pitch rate) from rigid-body dynamics, linearized at an operating point, and expressed in standard form. Our Structural Analysis examines eigenstructure, open-loop stability, and controllability/observability. We design state feedback by pole placement and LQR, add a Luenberger observer to address limited measurements (separation principle), and include integral action when zero steady-state error is required. We also utilize MATLAB/simulink to simulate and compare open- and closed-loop behavior by using step commands, torque disturbances, parameter variations, and actuator limits. The controllers stabilize the dynamics, increase damping, reduce settling time, and bound control effort within the linearized envelope. We summarize trade-offs between pole placement and LQR and note observer bandwidth versus noise sensitivity, which gives a clear reproducible pipeline from modeling to validation for launch-vehicle attitude control.**

***Index Terms*—Launch vehicles, Attitude control, Thrust vector control, State-space methods, LQR, Controllability, Observability**

I. Introduction

Accurate pitch-axis attitude control during ascent is essential for maintaining aerodynamic stability, meeting guidance pointing constraints, and rejecting thrust/atmospheric disturbances under tight actuator limits. Many modern launch vehicles achieve this by utilizing thrust-vector control (TVC) architectures that are required to operate reliably across changing flight conditions and hardware constraints [1], [2], [3], [4]. While the full 6-DoF dynamics are nonlinear, it is the case that near-upright segments admit a reliable small-angle linearization that enables transparent state-space analysis, controller synthesis (whether pole placement or LQR), and observer design via the separation principle [5], [6], [7]. Many recent integrated estimation control studies for small/suborbital launchers reinforce the practicality of linear designs around operating points [8].

a) Our Project Contributions: We aim to acheive the following objectives with this project:

- Derive a compact, linearized two-state model for pitch dynamics with TVC;
- Analyze open-loop eigenstructure, controllability, and observability;
- Synthesize State Feedback by pole placement and LQR.
- Validate Performance in MATLAB/Simulink under reference steps, disturbance torques, parameter variation, and actuator limits.

Our framing will follow widely adopted GN&C practice while still staying in the framework of the linear systems course toolkit we have learned in this course [1], [2], [5], [6], [7].

II. Related Works

So in order to understand the context in which we are working for this project, we conducted a small literature review within this area.

A. Launch Vehicle TVC and GN&C Practice

NASA and many other industry reports within the literature show ascent GN&C architectures employ Thrust-Vector Control (TVC) with stringent reliability requirements [1], [2]. Many control-allocation studies characterize actuator authority and gimbal mapping near the trim [3], while some classical analyses emphasize quantifying the minimum TVC capability that is required for booster stability during atmospheric flight [4]. Moreover, many GN&C requirement surveys within the literature emphasize robustness expectations and performance metrics [9] within their systems.

B. Linear State-Space Control and Observers

For regulation about fixed operating points, linear state-space methods supply transparent stability criteria and controller synthesis. In addition, linear quadratic regulator (LQR) balance performance and control effort, while Luenberger observers provide full-state estimates under limited measurements, in which it combines cleanly with feedback via the Separation Principle [5], [6]. In the literature, Integral-augmented LQ designs have been applied to ascent autopilots and motivate the 3-state controller that is utilized here [7].

C. Integrated Architectures and Loop Structures

Current studies in the literature on suborbital launchers demonstrate integrated estimation-control pipelines that are shown to be compatible with linearized models near operating points [8]. There are also exist comparative studies of single- versus two-loop autopilot-guidance design further the necessity for the modular control structure adopted here [10].

D. Summary

All of these references motivated our selection of a linearized-pitch-axis thrust-vector control (TVC) model and define the evaluation scenarios that we will use in our simulation setup and these methods are step-tracking, actuator-limited effort, disturbance rejection, and a $\pm 10\%$ robustness sweep.

III. Problem Formulation

Our objective for this problem is to regulate the pitch angle θ about an upright equilibrium, while satisfying time-domain specifications (i.e., settling time, overshoot, steady-state error) and actuator limits. Now, the signals that we are considering rely upon the states $\mathbf{x} = \begin{bmatrix} \theta & q \end{bmatrix}^\top$, an input $u = \delta$ (gimbal deflection), output $y = \theta$, reference is $r(t)$, and disturbance torque $d(t)$. In addition, the tracking error is given by the equation $e(t) = r(t) - y(t)$. In our project, we are using the linearized plant model is shown by the following equation:

$$\dot{x} = Ax + Bu + Ed, \qquad y = Cx, \tag{1}$$

where we will derive A, B, C, D in Section IV. Next, we will use an integral-augmented 3-state model. For one to obtain the zero steady-state error and a three-state design structure, we can define the integral of angle error, given by:

$$\xi(t) = \int_0^t (r(\tau) - \theta(\tau))\, d\tau,$$

and gives $\dot{\xi} = -\theta$ which is used for regulation. The augmented state $x_a = [\, \theta \; q \; \xi \,]^\top$ satisfy the following matrices:

$$A_a = \begin{bmatrix} 0 & 1 & 0 \\ -a & -b & 0 \\ -1 & 0 & 0 \end{bmatrix}, \qquad B_a = \begin{bmatrix} 0 \\ g \\ 0 \end{bmatrix}.$$

Finally, our design synthesizes the following:

1) Pole-Placement Control from desired second-order poles;
2) LQR control minimizing

$$\int (x^\top Q x + u^\top R u)\, dt$$

3) An optional Luenberger observer for solely $y = \theta$.

Now, let us go through how our system works.

IV. System Modeling

A. Physical Setup and Assumptions

We will consider a slender launch vehicle in a near-upright ascent, where pitch motion domintates and small-angle assumptions hold true. Thrust-Vector Control (TVC) generates a moment through a small gimbal deflection δ; define states θ (pitch angle) and $q = \dot{\theta}$ (pitch rate). The logic behind these physical assumptions and coordinate conventions follow standard practice within the current literature [11], [12].

1) Nonlinear Dynamics and Small-Disturbance Linearization: Newton-Euler rotation about the pitch axis gives $I_y \dot{q} = \tau_{\text{tvc}} + \tau_{\text{aero}} + d(t)$. For small nozzle angles, we use the equation $\tau_{\text{tvc}} \approx T \ell\, \delta \triangleq k_u u$ according to the literature [2], [3]. Now, the aerodynamic pitching moment linearizes to a spring-damper model, $\tau_{\text{aero}} \approx -k_\theta \theta - c_q q$, which is consistent with longitudinal short-period dynamics [11], [12]. If we divide by I_y gives the following linearized ODEs

$$\dot{\theta} = q, \quad \dot{q} = -a\theta - bq + gu + \tfrac{1}{I_y} d(t),$$

where it follows that $a = k_\theta / I_y$, $b = c_q / I_y$, and $g = k_u / I_y$. Now, we proceed to define our state-space form and transfer function.

B. State-Space Form and Transfer Function

With $x = [\, \theta \; q \,]^\top$ and $y = \theta$, it follows that:

$$A = \begin{bmatrix} 0 & 1 \\ -a & -b \end{bmatrix}, \quad B = \begin{bmatrix} 0 \\ g \end{bmatrix}, \quad C = \begin{bmatrix} 1 & 0 \end{bmatrix}, \quad E = \begin{bmatrix} 0 \\ 1/I_y \end{bmatrix}.$$

These matrices follow from a Jacobian evaluation of the nonlinear dynamics at the equilibrium [11], [13], [14]. With this in mind, we can determine our transfer function. The corresponding transfer function is defined by

$$G(s) = \frac{\Theta(s)}{U(s)} = \frac{g}{s^2 + bs + a},$$

as the standard second-order longitudinal form [12]. With all these considerations in mind, we can now move into our structural analysis.

V. Structural Analysis

A. Equilibrium and Linearization Validity

The upright operating point $(x, u) = (0, 0)$ corresponds to straight-up ascent where the pitch angle and pitch rate here are both zero. The linear model that we are utilizing in this project approximates the nonlinear vehicle dynamics accurately for small deviations in θ and q, which is the common practice in early-ascent GN&C. As demonstrated in [11], [12], this local linearity is valid so long as gimbal deflections remain small and aerodynamic moment slopes remain approximately constant. The characteristic polynomial of the open-loop plant, $p_{ol}(s) = s^2 + bs + a$, which indicates that aerodynamic parameters $a > 0$ restoring stiffness and $b > 0$ is damping yield a stable lightly damped second-order mode. In real-life applications, these parameters vary significantly during flight; moreover, the linear slice we consider correspond to a representative mid-ascent regime.

B. Eigenstructure and Natural Dynamics

The plant's eigenvalues are given by

$$\lambda_{1,2} = \frac{-b \pm \sqrt{b^2 - 4a}}{2},$$

which are used to determine short-period pitch motion. As a result, three important structural properties emerge:

1) **Weak Damping**: When $b^2 \approx a^2$, the system approaches critical damping. Many slender rockets have b relatively small, yielding lightly damped oscillations.
2) **Integrator-like Behavior**: If a, b are small (e.g., high altitudes with low aerodynamic authority), the system will behave like a double integrator. This will make stabilization impossible without control authority.
3) **Actuator-Dominated Regime**: When aerodynamic forces weaken, the value of $g = k_u/I_y$ become the dominant factor in controllability and bandwidth.

These properties will motivate feedback control to increase damping, reduce sensitivty to disturbances, and enforce performance specifications.

C. Controllability and TVC Authority

Our controllability matrix $\mathcal{C} = [B \;\; AB]$ is full rank for all $g \neq 0$ which guarantees that both states are directly influenced by the TVC actuator. Physically, g encapsulates the available control torque per unit gimbal angle. When g decreases, the closed-loop system becomes slower, and pole-placement designs require more aggressive gains. LQR formulations handle this more gracefully by penalizing control effort [15].

D. Observability and Sensor Limitations

With $C = \begin{bmatrix}1 & 0\end{bmatrix}$, only the pitch angle θ is directly measured. The observability matrix

$$\mathcal{O} = \begin{bmatrix} C \\ CA \end{bmatrix}$$

is full rank for non-pathological parameters, which enables a full Luenberger observer [15]. According to the literature, this is common practice in launch-vehicle GN&C where rate gyros may be unreliable or filtered at low bandwidths [6].

VI. Observer Design

Following classic state-estimation practice [5], [6], we utilize a full-order Luenberger Observer to reconstruct the measured pitch angle $y = \theta$:

$$\dot{\hat{x}} = A\hat{x} + Bu + L(y - C\hat{x}). \tag{2}$$

As established in Section V-B, the pair (A, C) is observable for generic (a, b), so L can be chosen to place the observer poles arbitrarily. To balance the fast decay of the estimation error with robustness to measurement noise, we adopt a standard GN&C guideline and place the observer eigenvalues $3-5\times$ faster than the dominant closed-loop poles. This ensures that $\tilde{x} = x - \hat{x}$, which converges on a shorter time scale than the controlled dynamics, while avoiding excessive noise amplification. By the separation principle [5], the controller gain K and observer gain L can be designed independently and then combined into an output-feedback realization.

VII. Simulation Setup and Results

To give a better real-world picture of the rocket, we employ the use of MATLAB.

A. Overview and Setup

In order to validate the controllers that are derived in Sections IV-V, we simulate the linearized pitch model introduced in (1). All our experiments use the matrices,

$$A = \begin{bmatrix} 0 & 1 \\ -a & -b \end{bmatrix}, \quad B = \begin{bmatrix} 0 \\ g \end{bmatrix}, \quad C = \begin{bmatrix} 1 & 0 \end{bmatrix}, \quad E = \begin{bmatrix} 0 \\ 1/I_y \end{bmatrix},$$

where these matrices were obtained by using the Newton-Euler derivation and small-angle linearization that was mentioned in Section III. When integral action is used, we employed the augmented model $\dot{x}_a = A_a x_a + B_a u$ with A_a, B_a being defined in Section II, and the state-feedback law, $u = -Kx_a$, where K is either the pole-placement or LQR gain from Section IV.

All of our simulations are carried out in MATLAB using $ode45$ over 10 seconds. Our experiments that we conduct in this project are motivated by the performance metrics emphasized in the launch-vehicle and linear-systems literature [4], [7], [11], [12].

B. Experiment 1: Step Tracking (Nominal Conditions)

This experiment will test the nominal closed-loop regulation using the linearized plant (A, B, C) of (1). A 2° reference step is applied, and the integral-augmented controller $u(t) = -Kx_a(t)$ is evaluated for both pole-placement and LQR gains.

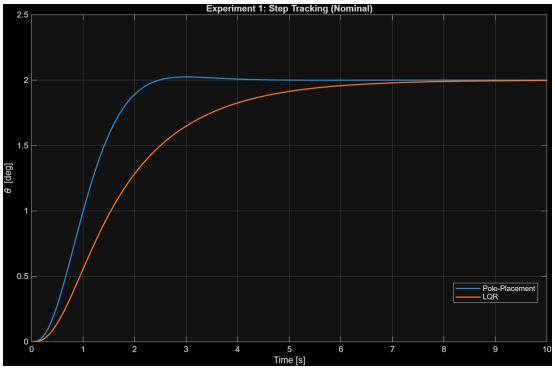

Fig. 1. Shows PP vs. LQR on a small step.

The above figure demonstrates two points. The first is that pole-placement yields faster convergence because the poles were assigned deeper in the left-half plane. On the other hand, linear-quadratic regulator (LQR) yields a smoother, lower-effort response consistent with minimizing

$$J = \int (x^\top Q x + u^\top R u)\, dt$$

derived earlier. This essentially verifies that the state-space controllers will stabilize the linear model and achieve the time-domain behavior that is predicted in the structural analysis section.

C. Experiment 2: Actuator Saturation

To test the limitations of the control input $u = \delta$, we repeat the step experiment with a larger 3° command and apply a saturation constraint given by $|u(t)| \leq u_{max}$, which is consistent with thrust-vector control (TVC) limits that are discussed in Borsody et al. [4]. Under saturation, we see that the effective dynamics deviate from the linear law $u = -Kx_a$, and thus the closed-loop system behaves like a forced version of the open-loop model $\dot{x} = Ax + Bu_{sat}$.

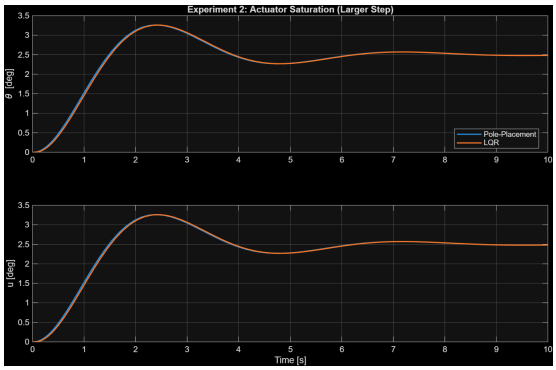

Fig. 2. Shows $\theta(t)$ and $u(t)$ with saturation clearly visible

From our above graph we can make two assumptions about the graph. Both controllers immediately reach the saturation limit, in which it produces nearly identical responses. In addition, the transient is slower because the system effectively reverts to the open-loop dynamics of A until the states move back into a controllable range. This shows that the actuator limits alter the behavior of the linearized control law.

D. Experiment 3: Disturbance Rejection

Next, we evaluate robustness to external torques, and we inject a disturbance $d(t) = 0.151_{[5,5.2]}(t)$ through the disturbance channel $Ed(t)$ in (1). It then follows that this directly perturbs the pitch rate equation $\dot{q} = -a\theta - bq + gu + 1/I_y d(t)$.

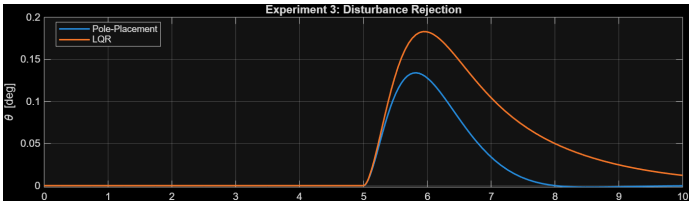

Fig. 3. Shows disturbance at $t \approx 5s$ and how both controllers recover.

From this figure, we observed three results. The first is that both controllers recover the equilibrium, which confirms closed-loop stability. Next, we saw that the pole-placement responds more aggressively, which is expected due to its pole locations. Finally, the Linear Quadratic Regulator (LQR) distributes its corrective effort more smoothly, which is consistent with the quadratic cost formulation. As a result, this behavior matches the disturbance-rejection patterns that were predicted in the eigenstructure discussion of Section IV.

E. Experiment 4: $\pm 10\%$ Parameter Variation

Real launch vehicles experience significant variation in aerodynamic stiffness a, damping b, and TVC authority g throughout ascent. To reflect this, we vary each plant parameter by $\pm 10\%$ and simulate the system using the same control law $u = -Kx_a$, but with altered matrices A, B. The perturbed plant becomes

$$A' = \begin{bmatrix} 0 & 1 \\ -(1 \pm 0.1)a & -(1 \pm 0.1)b \end{bmatrix}, \quad B' = \begin{bmatrix} 0 \\ (1 \pm 0.1)g \end{bmatrix}.$$

So we come to two conclusions based upon this graph and how it correlates with the literature.

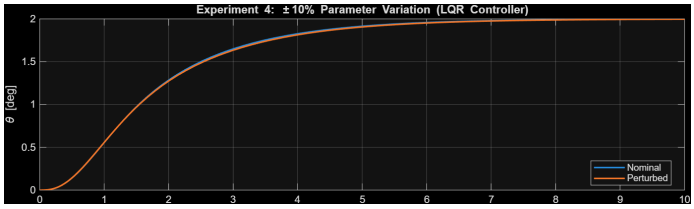

Fig. 4. Shows nominal vs perturbed tracking with very similar responses.

Firstly, the LQR controller's is robust to moderate parameter changes. Next, we saw that minimal sensitivity in both rise time and damping ratio.

VIII. Conclusion

Throughout this project, we developed and validated a linearized pitch-axis attitude control architecture for a launch vehicle operating near an upright ascent condition. We began by using Newton-Euler rotational dynamics, and then applied small-angle assumptions to derive the two-state model that is used throughout our analysis. The structural evaluation of this model confirmed stability, and observability, in which provided a theoretical foundation for state-space feedback and Luenberger observer design.

We used both pole-placement and LQR synthesis on an integral-augmented representation, in which we obtained controllers that satisfy the regulation and robustness objectives identified in the literature. The MATLAB simulations demonstrated that each controller stabilizes the vehicle, increases damping, and tracks reference commands while respecting actuator constraints. All four experimental scenarios (step tracking, actuator saturation, disturbance rejection, and parameter variation) collectively validated the behavior that was predicted from the analytic equations, which confirmed that the simplified linear model remains effective for representative ascent conditions.

In conclusion, our results showed that the linear state-space provide a transparent and reliable framework for early-ascent TVC. Despite the inherent nonlinearities of launch-vehicle dynamics, the linear slice captures the essential behavior that is required for for controller synthesis, and the LQR Design in particular exhibits strong robustness to modeling uncertainty. The workflow that we have developed here offers a reproducible pathway from physics-based modeling to controller

verification that aligns with industry GN&C practice and modern estimation-control integration.

References

[1] C. J. Dennehy, R. Lanzi, and P. Ward, "GN&C design overview and flight test results from NASA's max launch abort system (MLAS)," in *AIAA Guidance, Navigation, and Control Conference*, NASA NTRS 20110000768, 2010.

[2] B. Stuart, J. McEnulty, J. Wall, J. Orr, and P. Pektas, "Overview of the SLS core stage thrust vector control system design," in *AAS Guidance, Navigation and Control Conference*, NASA NTRS 20230001023, 2023.

[3] J. S. Orr and J. W. Wall, "Linear approximation to optimal control allocation for rocket nozzles with elliptical constraints," in *AIAA Guidance, Navigation, and Control Conference*, NASA NTRS 20110015708, 2011. DOI: 10.2514/6.2011-6500.

[4] J. Borsody and F. Teren, "Stability analysis and minimum thrust vector control requirements of booster vehicles during atmospheric flight," NASA, Tech. Rep. NASA TN D-4593, 1968.

[5] M. Athans, "The role and use of the stochastic linear-quadratic-gaussian problem in control system design," *IEEE Transactions on Automatic Control*, vol. AC-16, no. 6, pp. 529–552, 1971.

[6] D. G. Luenberger, "Observers for multivariable systems," *IEEE Transactions on Automatic Control*, vol. AC-11, no. 2, pp. 190–197, 1966. DOI: 10.1109/TAC.1966.1098323.

[7] T. Claggett and M. Langehough, "Application of integral-LQ to launch vehicle autopilot design," in *AIAA Guidance, Navigation, and Control Conference*, 1989. DOI: 10.2514/6.1989-3459.

[8] P. dos Santos and P. Oliveira, "Integrated architecture for navigation and attitude control of low-cost suborbital launch vehicles," *Acta Astronautica*, vol. 222, pp. 52–68, 2024. DOI: 10.1016/j.actaastro.2024.05.039.

[9] G. Di Mauro, M. Lawn, and R. Bevilacqua, "Survey on guidance, navigation and control requirements for spacecraft formation-flying missions," *Journal of Guidance, Control, and Dynamics*, vol. 41, no. 3, pp. 581–602, 2018. DOI: 10.2514/1.G002868.

[10] M. Levy, T. Shima, and S. Gutman, "Integrated single vs. two-loop autopilot-guidance design for dual-controlled missiles," in *2013 10th IEEE International Conference on Control and Automation (ICCA)*, Hangzhou, China, 2013, pp. 1730–1735. DOI: 10.1109/ICCA.2013.6564961.

[11] B. L. Stevens, F. L. Lewis, and E. N. Johnson, *Aircraft Control and Simulation: Dynamics, Controls Design, and Autonomous Systems*, 3rd ed. Wiley, 2015.

[12] M. V. Cook, *Flight Dynamics Principles: A Linear Systems Approach to Aircraft Stability and Control*, 3rd ed. Oxford: Butterworth-Heinemann, 2013, ISBN: 978-0-08-098242-7.

[13] I. Papp, "Missile mathematical model and system design," *AARMS*, vol. 16, no. 1, pp. 29–35, 2017. DOI: 10.32565/aarms.2017.1.3.

[14] A. B. Kisabo, F. A. Aliyu, O. C. Okwo, and S. O. Samuel, "State-space modelling of a rocket for optimal control system design," *Journal of Aircraft and Spacecraft Technology*, vol. 3, pp. 128–137, 2019. DOI: 10.3844/jastsp.2019.128.137.

[15] C.-T. Chen, *Linear System Theory and Design*, 4th ed. Oxford: Oxford University Press, 2013, ISBN: 9780199964543.